



Adaptive EKF-based ship trajectory estimation with earth curvature modeling and dynamic noise tuning

Berliana Elfada¹, Suci Awalia Gardara¹, Eddy Bambang Soewono¹, Yudi Widhiyasana¹

Informatics Engineering, Politeknik Negeri Bandung, Indonesia¹

Article Info

Keywords:

Earth's Curvature, Position Prediction, Extended Kalman Filter (EKF), Covariance Process and Measurement

Article history:

Received: July 04, 2025

Accepted: September 22, 2025

Published: February 01, 2026

Cite:

B. Elfada, S. A. Gardara, E. B. Soewono, and Y. Widhiyasana, "Adaptive EKF-Based Ship Trajectory Estimation with Earth Curvature Modeling and Dynamic Noise Tuning", *KINETIK*, vol. 11, no. 1, Feb. 2026.

<https://doi.org/10.22219/kinetik.v11i1.2397>

*Corresponding author.

Eddy Bambang Soewono

E-mail address:

ebang@polban.ac.id

Abstract

Accurate position estimation is critical for the effectiveness of automated weapon and navigation systems. Standard Extended Kalman Filter (EKF) models typically adopt flat-Earth assumptions and static noise covariances, which limit their accuracy in operational environments. This study proposes an optimized EKF framework that integrates two complementary approaches. First, ship trajectories are represented in Earth-Centered Earth-Fixed (ECEF) coordinates with a WGS-84 reference to account for Earth's curvature. Second, process (Q) and measurement (R) covariances are adaptively determined using Joint Likelihood Maximization (JLM) with logarithmic scale exploration, enabling the filter to automatically identify the most accurate configuration. Each Q/R setting is evaluated within the EKF framework using root mean square error (RMSE) derived from radar data logs. The method was tested under short-history scenarios (5 and 10 data points) within an operational range of ± 15 km, reflecting conditions commonly encountered in Combat Management Systems (CMS). The results show that while coordinate transformation alone provides only marginal improvements at short ranges, the combination of curvature modelling and adaptive Q/R tuning significantly reduces RMSE, achieving average errors approaching zero with high repeatability as measured by standard deviation. This research demonstrates a novel integration of geometric and statistical optimization in EKF design and highlights its applicability to ship trajectory estimation and defence systems.

1. Introduction

Accurate ship position estimation is fundamental to naval operations, supporting situational awareness and effective decision-making. A Combat Management System (CMS) relies on precise self-tracking and target trajectory prediction to ensure mission effectiveness and threat response. To achieve this, CMS integrates heterogeneous sensor sources such as radar, sonar, and GPS. However, these measurements are often degraded by noise, uncertainty, and environmental disturbances, highlighting a persistent challenge in obtaining reliable estimates. This limitation underscores the need for advanced filtering, sensor fusion, and adaptive estimation methods to address the growing complexity of maritime tracking tasks [1].

The Extended Kalman Filter (EKF) is widely adopted for trajectory estimation due to its capability to handle nonlinear system dynamics [2]. Compared to the linear Kalman Filter (KF), the EKF generally demonstrates superior performance [3]. In practice, EKF is often implemented in local East-North-Up (ENU) coordinate systems using a flat-Earth approximation. However, this approach introduces geometric distortions and cumulative errors that become significant in long-range or wide-area tracking. Furthermore, EKF performance is highly sensitive to the selection of process noise covariance (Q) and measurement noise covariance (R), which are typically assumed to be constant. This static assumption limits adaptability in dynamic maritime environments [4].

In the case of PT Len Industri, these challenges are particularly evident in the CMS platform. The EKF model currently employed still uses a two-dimensional approach without accounting for Earth's curvature, leading to significant discrepancies between predicted and actual ship positions in long-range operational scenarios. Furthermore, the filter applies static Q and R covariance matrices, neglecting environmental variability in the maritime domain, which further degrades prediction accuracy.

Several studies have investigated EKF variations across different application domains, and a comparative overview of these works alongside the present study is summarized in Table 1.

Table 1. Comparative Summary of Related Works and Proposed Method

Research Title	Discussion
Extended Kalman Filter Design and Motion Prediction of Ships using Live Automatic Identification System (AIS) Data	In this study, the Extended Kalman Filter (EKF) is employed to predict vessel trajectories based on Automatic Identification System (AIS) data. While AIS data are used as the primary input, the EKF is applied only within a local two-dimensional coordinate system, without considering the curvature of the Earth. Furthermore, the method relies on fixed (non-adaptive) Q and R covariance matrices [5].
Adaptive Kalman Filtering Methods for Low-Cost GPS/INS Localization for Autonomous Vehicles	This study develops an adaptive Extended Kalman Filter (EKF) to enhance the localization accuracy of autonomous vehicles equipped with low-cost GPS and INS sensors. The method operates in the Earth-Centered Earth-Fixed (ECEF) coordinate system and adaptively updates the Q and R covariance matrices based on residuals. However, the approach is intended for ground vehicles and does not address AIS data characteristics or vessel dynamics at sea [6].
Simulating Aerial Targets in 3D Accounting for the Earth's Curvature	This study models the trajectory of aerial targets in three-dimensional space using ECEF coordinates to account for the Earth's curvature. However, the research focuses solely on coordinate transformation and position dynamics in simulation, without implementing an adaptive EKF mechanism or adjusting the Q and R covariances [7].

In contrast to prior studies, this research integrates two complementary approaches: (1) accounting for Earth's curvature by converting polar coordinates into Earth-Centered Earth-Fixed (ECEF) coordinates, and (2) adaptively determining process (Q) and measurement (R) covariances through Joint Likelihood Maximization (JLM) with logarithmic scale exploration. Each Q/R configuration is evaluated within the Extended Kalman Filter (EKF) framework using Root Mean Square Error (RMSE) to identify the most accurate setting. This methodology aims to improve vessel position prediction in Combat Management System (CMS) tracking, where accuracy is vital for downstream functions such as target locking and weapon firing, which require high precision to prevent operational failure and ensure vessel safety [8], [9], [10]. The proposed approach has been implemented in the Application for Predictive Estimation (APE), developed in MATLAB and designed for future integration with the PT LEN Industri CMS simulation platform.

2. Research Method

This section describes the overall research design, algorithmic procedure, testing approach, and data acquisition process used in the development of the curvature-aware EKF prediction system with adaptive noise estimation.

2.1 Research Design

The research employs an experimental simulation strategy comprising the following steps:

1. Collection of radar log data (range, bearing, and ground speed).
2. Transformation of measurements from polar coordinates to Earth-Centered Earth-Fixed (ECEF) coordinates.
3. Application of the Extended Kalman Filter (EKF) with adaptive noise covariance tuning for trajectory prediction.
4. Evaluation of prediction accuracy using Root Mean Square Error (RMSE) and sigma metrics.

The evaluation compares baseline EKF under the flat-Earth approximation with the proposed curvature-aware EKF incorporating adaptive covariance tuning [11].

2.2 Data Preprocessing

This study utilizes recorded (non-live) radar log data as the primary input. Two observational configurations are applied: a five-point dataset, simulating conditions with minimal historical data for rapid decision-making, and a ten-point dataset, representing longer observation windows for improved stability. Each radar log entry contains three parameters:

- Bearing: the angle from the radar to the target ship relative to North.
- Range: the distance between the radar and the target ship.
- Groundspeed: the target ship's velocity over ground.

2.2.1 Data Transformation

1. The radar measurements in polar coordinates were first transformed into East-North-Up (ENU) coordinates using the formulation presented in Equation **Error! Reference source not found.** [12]:

$$\begin{aligned} X_{enu} &= range \cdot \cos(\varphi) \cdot \sin(\theta) \\ Y_{enu} &= range \cdot \cos(\varphi) \cdot \cos(\theta) \\ Z_{enu} &= range \cdot \sin(\varphi) \end{aligned} \quad (1)$$

where *range* is the distance between the radar and the ship's track point in polar coordinates, φ is the elevation angle (angle between the radar-to-target line and the local horizontal plane), and θ is the polar angle, defined by the orientation between the radar-to-North line and the radar-to-ship line.

2. The ENU coordinates were then converted to ECEF coordinates using the WGS-84 ellipsoid model, as shown in **Error! Reference source not found.**:

$$\begin{aligned} \begin{bmatrix} X \\ Y \\ Z \end{bmatrix} &= \begin{bmatrix} X_0 \\ Y_0 \\ Z_0 \end{bmatrix} + S^T \cdot \begin{bmatrix} X_{enu} \\ Y_{enu} \\ Z_{enu} \end{bmatrix} \\ \begin{bmatrix} v_X \\ v_Y \\ v_Z \end{bmatrix} &= S^T \cdot \begin{bmatrix} v_X^{enu} \\ v_Y^{enu} \\ v_Z^{enu} \end{bmatrix} \\ S &= \begin{bmatrix} -\sin & \cos\lambda & 0 \\ -\sin\phi\cos\lambda & -\sin\phi\sin\lambda & \cos\phi \\ \cos\phi\cos\lambda & \cos\phi\sin\lambda & \sin\phi \end{bmatrix} \end{aligned} \quad (2)$$

where $\begin{bmatrix} X_0 \\ Y_0 \\ Z_0 \end{bmatrix}$ represents the observer (radar) position in global ECEF coordinates, and $\begin{bmatrix} X_{enu} \\ Y_{enu} \\ Z_{enu} \end{bmatrix}$ represents the target position in 3D local coordinates, which is transformed to ECEF with the transposed rotation matrix S^T .

3. Geodetic conversion of radar position into Earth-Centered Earth-Fixed (ECEF) coordinates is performed prior to transforming the target's ENU coordinates (see Step 2). The observer's (radar) position is first expressed in ECEF coordinates as defined in Equations **Error! Reference source not found.** and **Error! Reference source not found.**:

$$N = \frac{a}{\sqrt{1 - e^2 \sin^2 \phi}} \quad (3)$$

$$\begin{aligned} X_0 &= (N + h) \cdot \cos\phi\cos\lambda \\ Y_0 &= (N + h) \cdot \cos\phi\sin\lambda \\ Z_0 &= (N(1 - e^2) + h)\sin\phi \end{aligned} \quad (4)$$

where N is the radius of curvature based on WGS-84 parameters, with semi-major axis $a = 6,378,137$ m and eccentricity $e^2 = 0.00669437999014$. The variables ϕ , λ , and h represent the observer's latitude, longitude, and height, respectively [13].

4. The conversion from ECEF coordinates to geodetic coordinates for the target vessel is expressed as follows:

$$\lambda = \text{atan2}(Y, X) \quad (5)$$

$$p = \sqrt{X^2 + Y^2} \quad (6)$$

$$\phi_0 = \tan^{-1}\left(\frac{Z}{p(1 - e^2)}\right) \quad (7)$$

$$h = \frac{p}{\cos\phi_0} - N \quad (8)$$

$$\phi = \tan^{-1}\left(\frac{Z}{p\left(1 - \frac{e^2 N}{N + h}\right)}\right) \quad (9)$$

$$\begin{aligned}\phi_{deg} &= \phi \times \frac{\pi}{180} \\ \lambda_{deg} &= \lambda \times \frac{\pi}{180}\end{aligned}\quad (10)$$

Equation **Error! Reference source not found.** determines the longitude, while Equation **Error! Reference source not found.** computes the horizontal projection distance p to the Z-axis, which provides an initial estimate of the latitude in Equation **Error! Reference source not found.**. Since no explicit formula exists for precise latitude and altitude estimation, the Newton-Raphson iteration is applied until convergence, resulting in the values given in Equations **Error! Reference source not found.** and **Error! Reference source not found.**. These calculations involve the Earth's radius of curvature defined in Equation **Error! Reference source not found.** [14]. Finally, Equation **Error! Reference source not found.** converts the latitude and longitude from degrees to radians.

5. Conversion of geodetic coordinates to global coordinates is performed as input for ship position prediction using the Extended Kalman Filter, employing the same mechanism described in Step 3.

2.3 Algorithm Design

The proposed method extends the Extended Kalman Filter (EKF) for ship trajectory estimation in Combat Management Systems (CMS). Given an initial state, an initial covariance, and radar measurements, the filter first adaptively estimates process (Q) and measurement (R) covariances using Joint Likelihood Maximization [15]. The EKF cycle then executes iteratively as follows:

1. Prediction step: Propagate the state and covariance using the motion model with acceleration input [16].
2. Update step: Compute the innovations, innovation covariance, Kalman Gain, and update the state and covariance [17].

As radar data are received, the prediction and update steps are repeated continuously. Accuracy is evaluated using Root Mean Square Error (RMSE), with the estimated trajectories benchmarked against radar data. The complete workflow is summarized in Figure 1. Adaptive covariance estimation aligns with previous work on dynamic system modelling under nonstationary conditions [18].

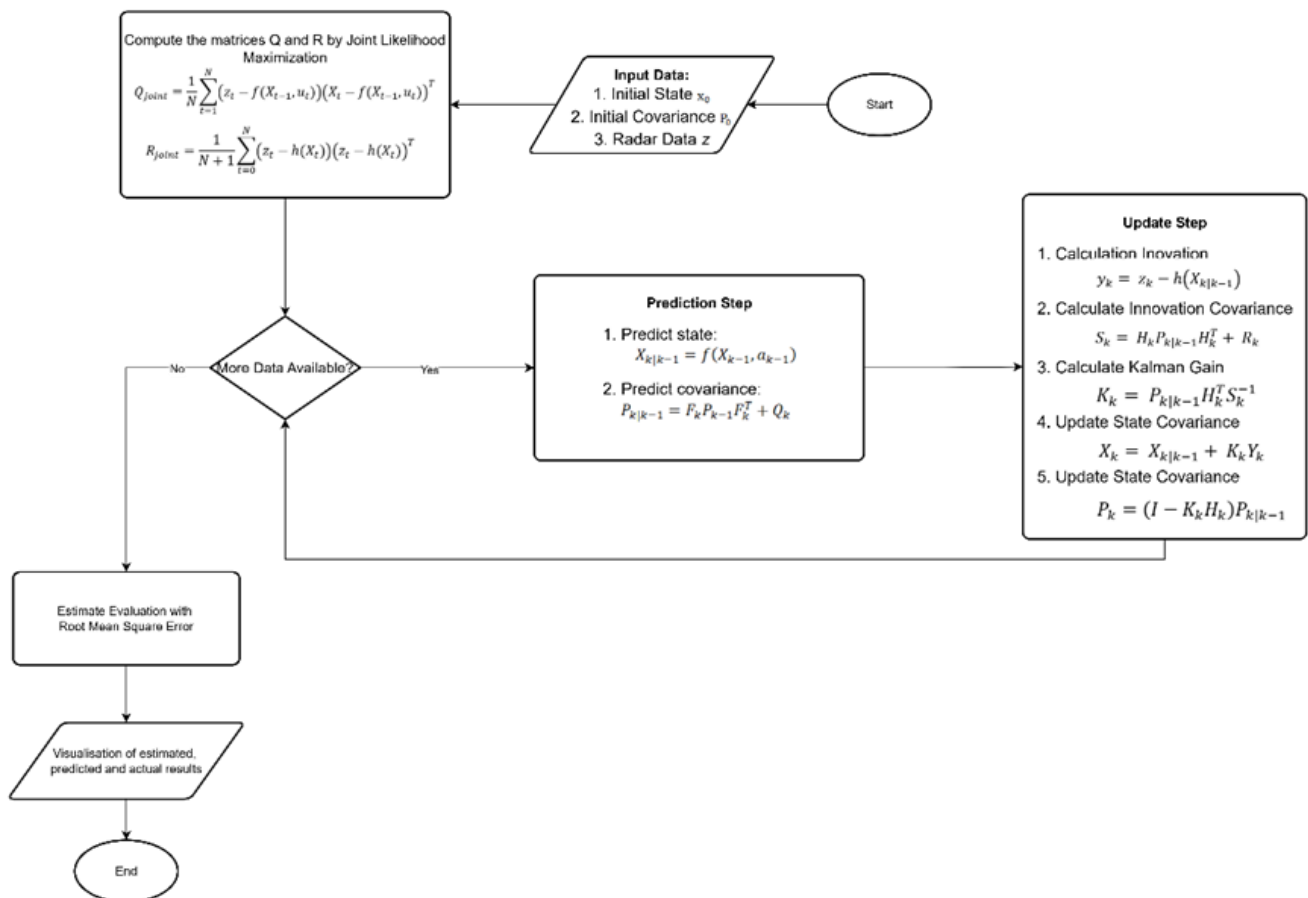


Figure 1. Algorithm EKF with Adaptive Q and R in ECEF

2.4 Mathematical Formulation

The motion model is nonlinear, and the state predictions are expressed as follows:

$$X_{k|k-1} = f(X_{k-1}, a_{k-1}) \quad (11)$$

$$P_{k|k-1} = F_k P_{k-1} F_k^T + Q_k \quad (12)$$

In the prediction stage, which is the first step in the Extended Kalman Filter (EKF), the system uses data from the previous time step $k - 1$ to estimate the state and its covariance at time k . Equations **Error! Reference source not found.** and **Error! Reference source not found.** represent the state transition function, the Jacobian matrix of the transition function, and the process noise covariance used in the state prediction and covariance propagation.

The measurement update equations are presented as follows:

$$y_k = z_k - h(X_{k|k-1}) \quad (1)$$

$$S_k = H_k P_{k|k-1} H_k^T + R_k \quad (2)$$

$$K_k = P_{k|k-1} H_k^T S_k^{-1} \quad (3)$$

$$X_k = X_{k|k-1} + K_k Y_k \quad (4)$$

$$P_k = (I - K_k H_k) P_{k|k-1} \quad (5)$$

In this step, the innovation is calculated as the difference between the actual radar measurement and the predicted measurement, as shown in Equation (1). The innovation covariance in Equation (2) combines the uncertainties of the state prediction and the measurement. The Kalman gain in Equation (3) determines the contribution of the measurement to the state update. The state estimate and its covariance are updated using Equations (4) and (5), respectively.

The residual-based adaptation of Q and R is given by:

$$Q_{joint} = \frac{1}{N} \sum_{t=1}^N (z_t - f(X_{t-1}, u_t))(X_t - f(X_{t-1}, u_t))^T \quad (6)$$

$$R_{joint} = \frac{1}{N+1} \sum_{t=0}^N (z_t - h(X_t))(z_t - h(X_t))^T \quad (7)$$

The process noise covariance matrix Q is estimated from the residual between the actual position data and the EKF-predicted position, while the measurement noise covariance matrix R is estimated from the residual between the radar measurements and the EKF-estimated measurements, as defined in Equations (6) and (7).

2.5 Testing and Evaluation

The performance of each EKF configuration was evaluated using two key metrics: Root Mean Square Error (RMSE) and standard deviation. These metrics were selected to assess both the accuracy and consistency of the position estimation results.

1. Performance was assessed using the Root Mean Square Error (RMSE), as defined in Equation 20:

$$RMSE = \sqrt{\frac{1}{N} \sum_{i=1}^N (\hat{y}_i - y_i)^2} \quad (8)$$

where \hat{y}_i represents the predicted value for the i -th observation, y_i is the actual value for the i -th observation, and N denotes the total number of observations. RMSE quantifies the mean magnitude of the estimation error, providing

a holistic measure of how close a predicted position is to the actual position. A smaller RMSE value indicates higher prediction accuracy and better overall model performance. In this investigation, RMSE is the main evaluation metric used to quantify the effectiveness of each EKF configuration in reducing prediction errors in different experimental conditions [19].

2. The standard deviation of the estimated positions across trials is presented in Equation (9):

$$s = \sqrt{\frac{\sum(r_i - \hat{r})^2}{n - 1}} \quad (9)$$

where r_i represents the data value at each position in the dataset, \hat{r} is the mean of all RMSE values, and n is the total number of observations. This metric quantifies the variability of the RMSE values across repeated experiments. A low standard deviation indicates that prediction errors are consistently close to the mean, implying stable model performance across different scenarios [20]. In contrast, a high standard deviation indicates significant variability in model accuracy between experimental runs. In this study, standard deviation should also be considered as a key indicator of consistency when comparing EKF models, particularly for the optimized method.

Testing was performed on two trajectory scenarios:

- 5-point trajectory test: Simulates rapid measurement acquisition under limited data conditions, representing situations requiring fast decision-making.
- 10-point trajectory test: Simulates extended measurement conditions, allowing for more stable estimations due to increased data availability.

Each EKF model configuration was tested multiple times to ensure result consistency. The baseline EKF model, which uses a flat earth coordinate system and static Q/R matrices, was compared against the proposed EKF model that incorporates Earth curvature via the ECEF coordinate system and applies dynamic Q/R tuning.

The proposed EKF variants were evaluated to assess the impact of ECEF transformation and adaptive noise covariance tuning on estimation performance. This testing framework was designed to validate whether curvature-aware modelling and dynamic noise adaptation significantly improve trajectory prediction accuracy under varying data availability conditions.

3. Results and Discussion

The experiments were conducted by applying the designed EKF configurations to both trajectory scenarios. This section presents the experimental results and the performance analysis of the different EKF configurations. Each experiment was performed using recorded radar data in two scenarios: 5-point and 10-point ship trajectories. Prediction performance was evaluated using Root Mean Square Error (RMSE) and standard deviation to assess estimation accuracy and consistency.

3.1 RMSE Evaluation

Three variants of EKF models were evaluated:

1. EKF-2D: standard EKF with flat-Earth assumption.
2. EKF-3D: EKF with ECEF coordinates transformation.
3. EKF-3D+QR: EKF with ECEF and adaptive Q/R tuning.

As shown in Table 2, the standard EKF-2D and EKF-3D models yielded nearly identical RMSE values, indicating that ECEF transformation alone did not significantly improve estimation accuracy. In contrast, the EKF-3D+Q/R model substantially reduced RMSE from tens of meters to sub-meter levels, achieving improvements of up to 86.6 m in individual test cases.

Table 2. Accuracy Difference between Standard EKF and Optimized EKF Number of Data Points: 5

EP Code	RMSE Standard EKF 2D (m)	RMSE EKF Optimized ECEF 3D (m)	RMSE EKF Optimized ECEF 3D + Adaptive QR (m)	Difference Standard EKF vs ECEF 3D	Difference Standard EKF vs ECEF 3D + Adaptive QR
EP1	83.0609	83.0609	0.9391	0.0001	82.1218
EP2	62.5292	62.5291	1.1065	0.0001	61.4227
EP3	83.8639	83.8639	1.0204	0.0000	82.8435
EP4	63.0982	63.0981	0.6087	0.0001	62.4895

EP5	87.3240	87.3239	0.7085	0.0001	86.6155
EP6	55.0447	54.8863	0.4190	0.1584	54.6257
EP7	61.0668	60.7799	0.6155	0.2869	60.4513
EP8	73.6226	73.3576	1.0871	0.2650	72.5355
EP9	57.1061	56.9240	0.4630	0.1821	56.6431
EP10	63.3584	63.2344	0.6449	0.1240	62.7135

With an increased number of observations, all models exhibited improved performance. However, the proposed method consistently outperformed the other configurations, reducing RMSE from tens of meters to below 1 meter, as shown in Table 3.

Table 3. Accuracy Difference between Standard EKF and Optimized EKF Number of Data Points: 10

EP Code	RMSE Standard EKF 2D (m)	RMSE EKF Optimized ECEF 3D (m)	RMSE EKF Optimized ECEF 3D + Adaptive QR (m)	Difference Standard EKF vs ECEF 3D	Difference Standard EKF vs ECEF 3D + Adaptive QR
EP1	63.1666	63.1666	0.6496	0.0000	62.5170
EP2	60.4398	60.4397	0.5476	0.0001	59.8922
EP3	66.9926	66.9925	0.4323	0.0001	66.5603
EP4	61.0467	61.0466	0.4344	0.0001	60.6123
EP5	41.6393	41.6393	0.2484	0.0000	41.3909

3.2 Standard Deviation Performance

To evaluate stability, the standard deviations of RMSE were analyzed across multiple test runs. The optimized ECEF 3D model with adaptive Q and R tuning consistently outperformed both the baseline 2D EKF and the non-adaptive 3D EKF, achieving deviations as low as 0.14 m (10 data points) to 0.29 m (5 data points). These results demonstrate highly stable and repeatable estimation performance, even under limited observations [21], [22]. In contrast, the baseline models exhibited substantially higher variability, with standard deviations consistently exceeding 9 m across scenarios. These findings are provided in Table 4.

Table 4. RMSE Standard Deviation Results

EKF Method	RMSE Standard Deviation (5 Data)	RMSE Standard Deviation (10 Data)
Standard EKF 2D	12.47	9.58
ECEF 3D	12.47	9.58
ECEF 3D + Adaptive QR	0.29	0.14

This dramatic improvement in standard deviation confirms that adaptive noise covariance tuning, when combined with curvature-aware modeling in ECEF coordinates, significantly enhances the filter's robustness and reliability, particularly in real-time naval tracking environments where rapid and accurate decision-making is critical.

3.3 Impact of Curvature vs. Adaptive Tuning

In theory, incorporating Earth's curvature through Earth-Centered Earth-Fixed (ECEF) coordinates should improve estimation accuracy, particularly in long-range tracking scenario [23]. However, the results in Table 2 indicate that the EKF-3D model, despite its higher complexity compared to EKF-2D, provided no significant accuracy gains and, in some cases, even increased the RMSE. This outcome is likely due to the limited dataset range (<50 km), where curvature effects are minimal. Similar findings have been reported in prior studies, where curvature corrections had little impact on short-range missile tracking but became relevant at extended ranges [24]. McLaughlin also noted that Earth curvature strongly affects radar coverage at long distances but is negligible in dense short-range radar networks [25]. These observations suggest that future work should evaluate scenarios beyond 50 km to fully assess the contribution of curvature modeling in trajectory estimation.

3.4 Impact of adaptive Q and R Tuning

Through adaptive tuning of the process noise (Q) and measurement noise (R), the system dynamically adjusted to variations in ship motion and radar uncertainty [26], [27]. This mechanism enabled EKF-3D+QR model to:

1. Rely more on radar measurements when model predictions were uncertain (high Q), and
2. Rely more on model predictions when radar data were noisy (high R).

This approach significantly reduced RMSE, with some estimates approaching zero error, thereby improving both the accuracy and adaptability of the system.

3.5 Visualization of Trajectory Estimation

Figure 2 and Figure 3 present a 3D visualization of the ship trajectories in the Earth-Centered Earth-Fixed (ECEF) coordinate system. The red line represents the actual radar data, while the blue line shows the trajectory estimated by the Extended Kalman Filter (EKF) with Earth curvature modelling, and the green line illustrates the forward-time prediction of the ship's future trajectory based on the EKF model. The predicted trajectories closely follow the actual paths and largely overlap across most segments, with only minor deviations at a few points. This indicates good convergence between the predicted and actual trajectories.

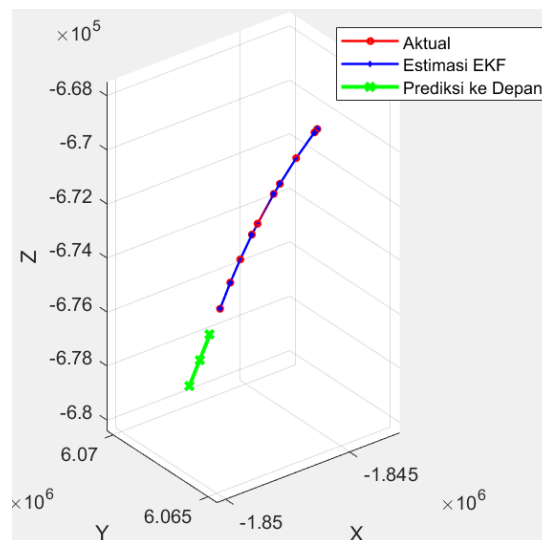


Figure 2. Visualization of Comparison Between Actual and Predicted (10 data)

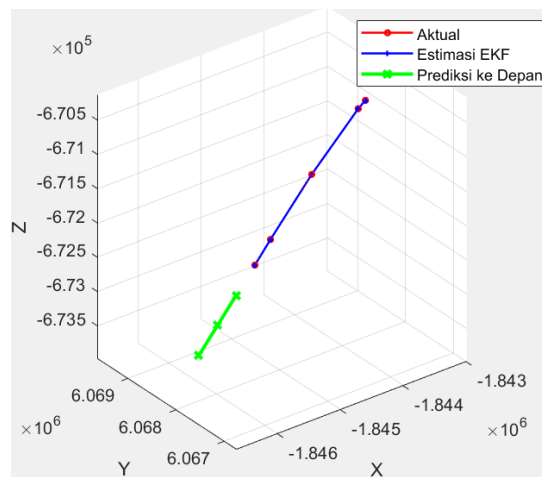


Figure 3. Visualization of Comparison Between Actual and Predicted (5 data)

4. Conclusion

This research investigated and optimized the Extended Kalman Filter (EKF) approach to enhance ship position estimation accuracy in maritime tracking systems. The proposed method transforms the model from a 2-dimensional (2D) flat-Earth coordinate system to a 3-dimensional Earth-Centered Earth-Fixed (ECEF) framework [28], while

incorporating adaptive tuning of the process and measurement noise covariance matrices (Q and R). The main findings are summarized as follows:

1. Transformation from 2D to 3D ECEF coordinates resulted in minimal accuracy gains, as Earth curvature effects were negligible within the tested short-range dataset (~15 km).
2. Adaptive tuning of Q and R matrices significantly improved prediction accuracy, reducing RMSE by 60-80 m compared to the baseline EKF-2D and maintaining final trajectory errors consistently below 1 m.
3. The enhanced EKF model demonstrated high robustness, with standard deviations reaching as low as 0.14 across multiple test conditions.
4. The results confirm that adaptive noise covariance tuning has a greater impact on predictive accuracy than coordinate transformation alone.
5. Since the experimental scenarios covered only a ± 15 km range, the effect of Earth curvature could not be fully validated. Future studies should include longer-range test scenarios (e.g., >50 km) to better evaluate the significance of curvature modeling in trajectory estimation.

Acknowledgement

The authors would like to thank PT Len Industri and Bandung State Polytechnic for providing research support and facilities throughout this study. The implementation code used in this research is publicly available at <https://github.com/suciawalia/ship-trajectory-estimation-EKF.git>

References

- [1] Q. A. M. Thi, C. Lee, T. M. Tao, and C. H. Youn, "Tracking Vessel Activities with AIS Data using an Adaptive Extended Kalman Filter," *International Conference on ICT Convergence*, pp. 349–354, 2024. <https://doi.org/10.1109/ICTC62082.2024.10827762>
- [2] C. Yang, Z. Gao, X. Huang, and T. Kan, "Hybrid extended-cubature Kalman filters for non-linear continuous-time fractional-order systems involving uncorrelated and correlated noises using fractional-order average derivative," *IET Control Theory and Applications*, vol. 14, no. 11, pp. 1424–1437, 2020. <https://doi.org/10.1049/iet-cta.2019.1121>
- [3] M. S. Grewal and A. P. Andrews, *Kalman Filtering -- theory and practicing using matlab -- edisi 3*, 3rd ed. 2008.
- [4] A. Wondosen, Y. Debele, S. K. Kim, H. Y. Shi, B. Endale, and B. S. Kang, "Bayesian Optimization for Fine-Tuning EKF Parameters in UAV Attitude and Heading Reference System Estimation," *Aerospace*, vol. 10, no. 12, 2023. <https://doi.org/10.3390/aerospace10121023>
- [5] S. Fossen and T. I. Fossen, "Extended kalman filter design and motion prediction of ships using live automatic identification system (AIS) Data," *Proceedings - 2018 2nd European Conference on Electrical Engineering and Computer Science, EECS 2018*, no. December, pp. 464–470, 2018. <https://doi.org/10.1109/EECS.2018.00092>
- [6] A. Werries and J. M. Dolan, "Adaptive Kalman Filtering Methods for Low-Cost GPS / INS Localization for Autonomous Vehicles," pp. 1–9, 2016.
- [7] D. F. Crouse, "Simulating aerial targets in 3D accounting for the earth's curvature," *Journal of Advances in Information Fusion*, vol. 10, no. 1, pp. 31–57, 2015.
- [8] B. Or and I. Klein, "A Hybrid Model and Learning-Based Adaptive Navigation Filter," *IEEE Trans Instrum Meas*, vol. 71, no. Dvl, pp. 1–11, 2022. <https://doi.org/10.1109/TIM.2022.3197775>
- [9] B. Cole and G. Schamberg, "Unscented Kalman filter for long-distance vessel tracking in geodetic coordinates," *Applied Ocean Research*, vol. 124, 2022. <https://doi.org/10.1016/j.apor.2022.103205>
- [10] B. Boulkroune, K. Geebelen, J. Wan, and E. van Nunen, "Auto-tuning extended Kalman filters to improve state estimation," *IEEE Intelligent Vehicles Symposium (IV)*, 2023.
- [11] M. Sato and M. Toda, "Adaptive Algorithms of Tuning and Switching Kalman and H^∞ Filters and Their Application to Estimation of Ship Oscillation with Time-Varying Frequencies," *IEEE Transactions on Industrial Electronics*, 2019.
- [12] S. Zollo and B. Ristic, "On polar and versus Cartesian coordinates for target tracking," *ISSPA 1999 - Proceedings of the 5th International Symposium on Signal Processing and Its Applications*, vol. 2, no. February 1999, pp. 499–502, 1999. <https://doi.org/10.1109/ISSPA.1999.815719>
- [13] A. Budiyono, "Principles of GNSS, Inertial, and Multi-sensor Integrated Navigation Systems," *Industrial Robot: An International Journal*, vol. 39, no. 3, 2013. <https://doi.org/10.1108/ir.2012.04939caa.011>
- [14] K. N. Baasch, L. Icking, F. Ruwisch, and S. Schön, "Coordinate Frames and Transformations in GNSS Ray-Tracing for Autonomous Driving in Urban Areas," *Remote Sens (Basel)*, vol. 15, no. 1, 2023. <https://doi.org/10.3390/rs15010180>
- [15] P. Abbeel, A. Coates, M. Montemerlo, A. Y. Ng, and S. Thrun, "Discriminative Training of Kalman Filters," *J Neurochem*, vol. 52, no. 5, pp. 1401–1406, 2005.
- [16] A. Li and Z. Qiang, "Multi-sensor data fusion method based on adaptive Kalman filtering," 2024, pp. 306–311. <https://doi.org/10.1145/3638782.3638829>
- [17] Y. Chen, W. Li, and Y. Wang, "Online Adaptive Kalman Filter for Target Tracking With Unknown Noise Statistics," vol. 5, no. 3, 2021. <https://doi.org/10.1109/LSSENS.2021.3058119>
- [18] Q. Dong, N. Wang, C. Zou, and L. H. K. Qu, "An Adaptive Order Variation Mathematical Modeling of Ship Maneuvering Motion Under Environmental Changes," 2024. <https://doi.org/10.1109/OCEANS51537.2024.10682352>
- [19] L. Tian, W. Xue, and L. Cheng, "Hand Position Tracking based on Optimized Consistent Extended Kalman Filter," 2022. <https://doi.org/10.1109/CCDC55256.2022.10033812>
- [20] H. S. Darling, "Do you have a standard way of interpreting the standard deviation? A narrative review," *Cancer Research, Statistics, and Treatment*, vol. 5, no. 4, pp. 728–733, 2022. https://doi.org/10.4103/crst.crst_284_22
- [21] S. Hu and B. Yan, "Ship Tracking with Static Electric Field Based on Adaptive Progressive Update Extended Kalman Filter," *MATEC Web of Conferences*, vol. 232, pp. 1–4, 2018. <https://doi.org/10.1051/mateconf/201823204063>
- [22] F. Deng, H.-L. Yang, and L.-J. Wang, "Adaptive Unscented Kalman Filter Based Estimation and Filtering for Dynamic Positioning with Model Uncertainties," *Int J Control Autom Syst*, vol. 117, pp. 667–687, 2019. <https://doi.org/10.1007/s12555-018-9503-4>
- [23] C. Jia, J. Ma, and W. M. Kouw, "Multiple Variational Kalman-GRU for Ship Trajectory Prediction with Uncertainty," vol. 61, no. 2, 2025. <https://doi.org/10.1109/TAES.2024.3491053>

- [24] W. Lv, L. Wang, and S. Jiang, "A Trajectory Simulation Model of the Short-Range Anti-ship Missile Based on Considering Curvature of the Earth," 2010. <https://doi.org/10.1109/ICCMS.2010.444>
- [25] D. J. McLaughlin, "Gap free CONUS surveillance using dense networks of short range radars," 2010. <https://doi.org/10.1109/ARRAY.2010.5613393>
- [26] T. Zou, W. Zeng, W. Yang, M. C. Ong, and Y. W. W. Situ, "An Adaptive Robust Cubature Kalman Filter Based on Sage-Husa Estimator for Improving Ship Heave Measurement Accuracy," *IEEE Sens J*, vol. 23, no. 9, 2023. <https://doi.org/10.1109/JSEN.2023.3260300>
- [27] B. Ge, H. Zhang, L. Jiang, Z. Li, and M. M. Butt, "Adaptive unscented kalman filter for target tracking with unknown time-varying noise covariance," *Sensors (Switzerland)*, vol. 19, no. 6, 2019. <https://doi.org/10.3390/s19061371>
- [28] G. Yu, C. Li, and B. Lu, "Processing 3D Flight Trajectory Data with Adaptive Kalman Filtering," 2024. <https://doi.org/10.1109/ICCASIT62299.2024.10828030>